Journal of Physiology (1989), **408**, *pp.* 313–332
With 10 text-figures
Printed in Great Britain

DUAL EFFECTS OF INTRACELLULAR MAGNESIUM ON MUSCARINIC POTASSIUM CHANNEL CURRENT IN SINGLE GUINEA-PIG ATRIAL CELLS

BY MINORU HORIE* AND HIROSHI IRISAWA

From the National Institute for Physiological Sciences, Myodaiji, Okazaki 444, Japan

(*Received 29 February 1988*)

SUMMARY

1. The effects of internal Mg^{2+} ions on the muscarinic acetylcholine (ACh) receptor-mediated K^+ currents were investigated in single atrial cells of guinea-pigs, using the whole-cell and inside-out modes of the patch-clamp technique.

2. During cell dialysis in the whole-cell-clamp condition, the depletion of internal Mg^{2+} increased outward muscarinic K^+ currents but decreased inward currents, thereby reducing the inwardly rectifying property of the channels.

3. When inside-out patches were prepared, channel availability was abolished and was reactivated by internal application of guanosine 5′-triphosphate (GTP) or its non-hydrolysable analogue, 5′-guanylyl imidodiphosphate (GppNHp), in the presence of Mg^{2+}. GppNHp led to a recovery of the channels also in the nominal absence of Mg^{2+} ($0[Mg^{2+}]_i$).

4. The activation of single-channel currents by intracellular GTP and Mg^{2+} was dose-dependent. Both concentration–response curves were fitted by saturation kinetics with Hill coefficients of 1, and the half-maximum doses were 24 ± 8 μM for GTP and 67 ± 14 μM for Mg^{2+}. The effects of Mg^{2+} on activation of K^+ currents were additive with those of GTP, suggesting the presence of two independent binding sites for GTP and Mg^{2+}.

5. The single-channel conductance became virtually ohmic when measured at nominally zero $[Mg^{2+}]_i$ while GppNHp was used to recover the channel activity. Micromolar $[Mg^{2+}]_i$ reduced the unitary amplitude of single open-channel currents in a dose- and voltage-dependent manner, showing half-blocking doses of 293 μM at +40 mV and 115 μM at +60 mV.

6. Voltage-dependent kinetics of Mg^{2+} block were described using equations based on Eyring rate theory (Woodbury, 1971; Hille, 1984), where the coefficient for voltage dependence (δ) was 0·63.

7. Intracellular Mg^{2+}, at a physiological concentration, has a dual action on the muscarinic K^+ channel: first Mg^{2+} activates the channel in the presence of GTP through GTP-binding proteins (G proteins), and secondly it blocks outward currents through the channel, thereby causing the inwardly rectifying property.

* Present address: The Third Department of Internal Medicine, Kyoto University, School of Medicine, Kyoto 606, Japan.

INTRODUCTION

Acetylcholine (ACh) is known to increase the inwardly rectifying K^+ conductance (muscarinic K^+ channel) of pacemaker or atrial cells and cardiac Purkinje fibres. It hyperpolarizes the resting membrane and suppresses the pacemaker depolarization, thereby causing a bradycardia (Hutter & Trautwein, 1956; Garnier, Nargeot, Ojeda & Rougier, 1978; Noma & Trautwein, 1978; Noma, Pepper & Trautwein, 1979; Mubagwa & Carmeliet, 1983; Iijima, Irisawa & Kameyama, 1985; Carmeliet & Mubagwa, 1986*a b*). Unitary current measurements in cell-attached patches have also shown that inward current through the muscarinic K^+ channel flows much more easily than outward current (Sakmann, Noma & Trautwein, 1983; Soejima & Noma, 1984). Mechanisms underlying the inward rectification of this channel are not well understood. Unidirectional and voltage-dependent Mg^{2+} block has been found to underlie the inward rectification of adenosine triphosphate (ATP)-sensitive K^+ channels and of inwardly rectifying K^+ channels of mammalian cardiac cells (Horie, Irisawa & Noma, 1987; Findlay, 1987*a*; Matsuda, Saigusa & Irisawa, 1987; Vandenberg, 1987). Recently, a similar Mg^{2+} block has also been noted in the inwardly rectifying muscarinic K^+ channels (Horie & Irisawa, 1987).

On the other hand, GTP-binding proteins (G proteins) have been shown to couple the muscarinic receptors to the K^+ channels in mammalian atrial cells (Pfaffinger, Martin, Hunter, Nathanson & Hille, 1985; Breitwieser & Szabo, 1985), where activation of channels requires internal Mg^{2+} (Kurachi, Nakajima & Sugimoto, 1986; Horie & Irisawa, 1987). If internal Mg^{2+} blocks the channel as was noted in other cardiac K^+ channels, no outward current would flow despite the higher availability of the channel at a higher concentration of intracellular Mg^{2+}. Conversely, without internal Mg^{2+}, there might not be any channel activation.

There is little quantitative information on this dual role of internal Mg^{2+} in the regulation of muscarinic K^+ current. In the present work, the effects of $[Mg^{2+}]_i$ on the conductance and activation properties of muscarinic K^+ channels were examined at both macroscopic and microscopic current levels.

METHODS

Preparations

Guinea-pigs of either sex (200–400 g) were anaesthetized with intraperitoneal injections of sodium pentobarbitone (30 mg/kg). The chest was opened and the aorta was cannulated *in situ*. The heart was then dissected out and a Langendorf perfusion was started with a normal Tyrode solution (Table 1) to wash out the blood. The perfusate was then switched to a nominally Ca^{2+}-free Tyrode solution (about 50 ml) followed by 0·05 mM-Ca^{2+} Tyrode solution (50 ml) containing 0·4 mg/ml collagenase (Sigma, type I), which was recirculated for 10–15 min with a peristaltic pump. The collagenase was then washed out by perfusing with about 100 ml of high-K^+, low-Cl^- solution (Isenberg & Klöckner, 1982). The temperature of all solution was kept at 35–37 °C. Perfusates were equilibrated with O_2 during the Langendorf perfusion. Atria were then isolated, gently chopped and stirred within 20 ml of high-K^+, low-Cl^- solution. The cell suspension was passed through a stainless-steel filter (diameter 65 μM). The sedimented cells were washed several times with high-K^+, low-Cl^- solution (about 30 ml) to eliminate the collagenase. The final cell suspension was pre-incubated for at least 60 min at 4 °C prior to the experiments. A few drops of cell sediment were then dispersed into the chamber (0·5 ml) filled with Tyrode solution on the stage of an inverted microscope. After long spindle-shaped single atrial cells attached firmly to the bottom of the

TABLE 1. Composition of solutions

	Tyrode Solutions					
	NaCl	NaH_2PO_4	KCl	$CaCl_2$	$MgCl_2$	HEPES
Normal	136·5	0·3	5·4	1·8	0·5	5
Ca^{2+}-free	136·5	0·3	5·4	—	0·5	5

	Whole-cell pipette solutions					
Potassium asparate	KCl	K_2ATP	$MgCl_2$	EGTA	HEPES	K_2CrP
100	20	5	0–1	10	5	5

	Single-channel pipette solutions		
	KCl	$CaCl_2$	Acetylcholine	HEPES
	150	1·8	0·001–0·005	5

	Internal solutions (for inside-out patches)				
	KCl	Na_2GTP	Mg_2SO_4	EGTA	HEPES
Standard	150	—	—	1	5
Test solutions	150	0·002–2	0·003–4	1	5

EGTA, ethyleneglycol-bis(β-aminoethylether)*N*,*N*′-tetracetic acid (Dotide); HEPES, *N*-2-hydroxyethylpiperazine-*N*′-2-ethanesulphonic acid (Dotide); CrP, creatine phosphate (Sigma).

recording chamber, the Tyrode solution was superfused by gravity (1·5 ml/min, 30–35 cmH_2O) for at least 15 min before starting electrophysiological experiments. Only quiescent cells showing a clear cross-striation, without granules and blebs, were used. The resting potential of single atrial cells in 5·4 mM-K^+ Tyrode solution was assumed to be −79 mV (Iijima *et al.* 1985).

Solutions and drugs

The compositions of external and internal solutions for whole-cell or single-channel current recordings are summarized in Table 1. To prepare solutions containing a desired concentration of free Mg^{2+} (Mg^{2+} test solutions), an appropriate amount of $MgSO_4$ was added to the standard internal solutions (Table 1, for inside-out patches) or to the pipette solutions, according to Fabiato & Fabiato (1979) with correction by Tsien & Rink (1980). The pH of all solutions was adjusted to 7·4 with HEPES–KOH or NaOH buffer. Acetylcholine chloride (Sigma), D600 (Knoll), guanosine 5′-triphosphate (GTP: Yamasa Inc., Japan), and 5′-guanylyl imidodiphosphate (GppNHp: Boeringer) were used.

Whole-cell clamp and cell dialysis

Patch pipettes were fabricated from thin-walled glass capillary tubes (Mercer Glass Works, NY, USA), and were fire-polished. Pipettes had tip diameters of 3–4 μm and resistances of 2–3 MΩ when filled with the solutions described above. The methods used to measure whole-cell currents during cell dialysis were as previously reported (Matsuda & Noma, 1984). Briefly, after the gigaohm seal was established at the centre of the atrial cell using a patch electrode containing normal Tyrode solution (Table 1), the pipette solution was changed to the high-K^+ test solution supplied from plastic reservoirs (about 1 ml in volume) via a fine polyethylene inlet by applying a negative pressure of 20–30 cmH_2O. The tip of the inlet was about 50 μm in internal diameter, and reached within 150 μm of the tip of the patch electrode (exchange rate approximately 50 μl/min) (Fig. 1*A*). By then increasing the negative pressure, the cell membrane beneath the patch electrode was broken, so that a whole-cell configuration of the patch clamp was obtained.

Modified inside-out patch-clamp technique

To obtain cell-free patches (Hamill, Marty, Neher, Sakmann & Sigworth, 1981), the open-cell-attached patch method (Horie *et al.* 1987) was modified. The gigaohm seal was established near the centre of a single atrial cell with a Sylgard-coated glass pipette of resistance 4–5 MΩ when filled with the various solutions, and the superfusate was then changed to a nominally Ca^{2+}-free Tyrode

solution for 2–3 min followed by a standard 150 mM-K^+ internal solution (Table 1), to help prevent contraction during depolarization. Then, using another glass pipette mounted on a separate manipulator, the cell membrane was gently pressed against the bottom of the recording chamber. The recording electrode was then pulled up, and the cell-free inside-out patch mode was established at almost every trial when a tight seal of patch pipette had been obtained. The inside-out condition was confirmed by observing an abrupt disappearance of channel events, which had shown marked openings during cell-attached recording (Fig. 3). The tips of the pipettes for pressing against the cell were much larger than those used for recording (aperture 100–150 μm). The former pipettes were filled with a standard internal solution containing 1 mM-EGTA and were later used for drug application.

Application of drugs

The tip of the glass pipette used to press against the cell was subsequently positioned about 100 μm upstream of the recording pipette as illustrated in Fig. 1*A*. The method of rapid and selective application of drugs resembled those described by Yellen (1982) and Dunne & Petersen (1986). The flow rate through the pipette was about 1 ml/min, and solutions were exchanged smoothly by switching a valve connected to the top of the glass pipettes (Fig. 1*A*). To avoid mixing of the test and bath solutions, the latter solution was simultaneously superfused at a constant rate of 1–1·5 ml/min. The same method was also used for application of ACh during the whole-cell clamp (Fig. 1*A*). The bath was grounded through an agar/Ag–AgCl bridge. All experiments were performed at room temperature (22–24 °C).

Data analysis

Whole-cell and single-channel currents were recorded using a patch-clamp amplifier (List Electronics, EPC7) and stored on videotape through a pulse-code modulation system (NF Circuit RP880) for later analysis with computers (Hitachi E600 and NEC PC98XA). Single-channel currents were sampled every 0·1–0·5 ms via a Bessel-type low-pass filter (48 dB octave^{-1} with cut-off frequency of 3 kHz, NF Circuit, FV-625A). Currents were then divided into segments of baseline (no channels open) and those of open-channel current. The average was calculated for each group of segments, and mean patch current ($\bar{i}$) was estimated as the difference of the two averages. The unitary amplitude of open-channel current (i) was measured as the difference of averaged patch current between the baseline and the open state at the first level. Segments of baseline were always obtained before internal application of guanine nucleotides.

RESULTS

Macroscopic ACh-induced currents under control of intracellular Mg^{2+}

Figure 1*B* illustrates the effects of ACh in the presence and absence of GTP. When the whole-cell clamp mode was made using a pipette solution containing neither GTP nor Mg^{2+}, exposure to 10^{-7} M-ACh failed to evoke current activation (arrow above the upper trace). After the pipette solution was changed to one containing 0·2 mM-GTP and 0·5 mM-Mg^{2+}, the current level at a holding potential of −40 mV began to progressively increase. These findings agree with those obtained in previous studies on cardiac myocytes and suggest that both intracellular GTP and Mg^{2+} are necessary to transduce ACh-receptor stimulation to the channel effector (Pfaffinger *et al.* 1985; Breitwieser & Szabo, 1985; Sorota, Tsuji, Tajima & Pappano, 1985; Kurachi *et al.* 1986).

The outward holding current at −40 mV then began to decline to reach a new steady state in 12 min, despite the continued presence of 10^{-7} M-ACh (desensitization: note interruption of the trace in the lower panel of Fig. 1*B*). When Mg^{2+} was then eliminated from the patch pipette, the outward current showed a transient increase within 2 min, followed by a decrease. On removing Mg^{2+}, outward currents elicited

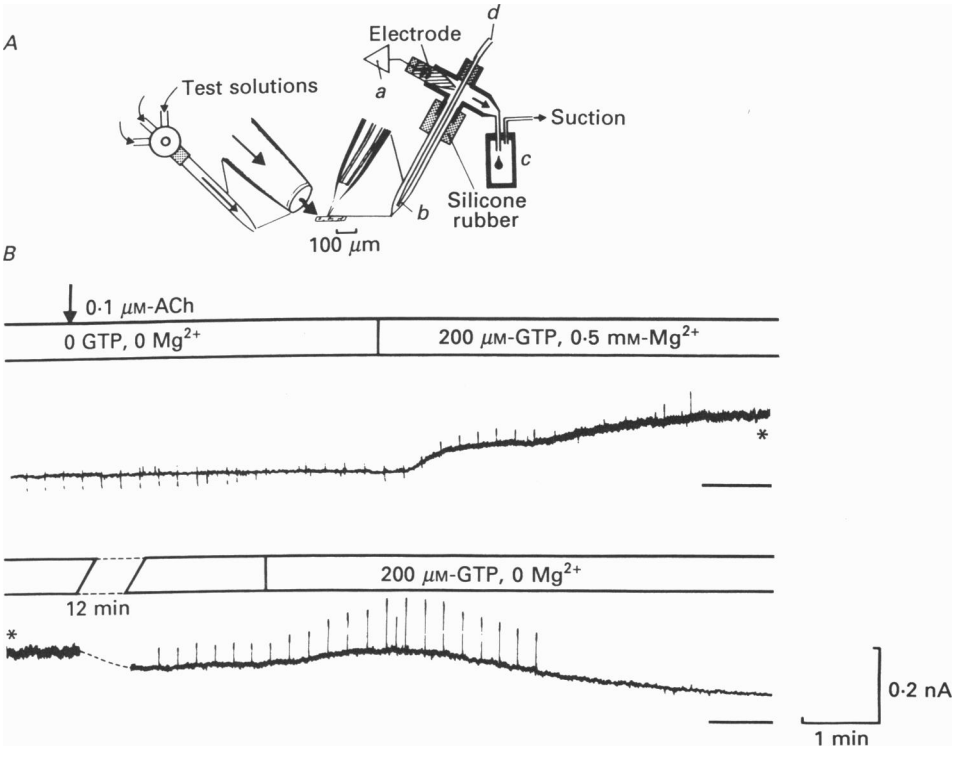

Fig. 1.*A*, experimental design to apply various test solutions and to dialyse the cell interior. A wide-tipped glass pipette was positioned $\sim 100\ \mu m$ upstream of the cell attached to the recording pipette so that the perfusate could be changed promptly (left part of scheme). The agar bridge to the clamp amplifier (*a*), glass electrode (*b*), the reservoir for waste fluid (*c*) and conduit for test solutions (*d*) were connected to the four-way plastic valve. Negative pressure was applied to this reservoir (20–30 cmH_2O, right part of the diagram). The middle part shows the magnified view of the cell and the tip of the electrode. *B*, membrane current at the holding potential of −40 mV in symmetrical 150 mM-K^+ solutions; asterisks indicate that the tracings are continuing. The arrow indicates the time when ACh is applied to the cell. After this time, 0·1 μM-ACh is present throughout the remainder of the recording. The content of the pipette solution is indicated above the current traces. Before ACh application, more than 10 min has elapsed after the development of the whole-cell clamp condition with 0 mM-GTP and nominally Mg^{2+}-free pipette solution. The dashed lines in the lower panel indicate a 12 min intermission of record. In the lower trace, depolarizing pulses to −10 mV were applied every 15 s. The horizontal bars to the right of each trace show the zero current level.

by depolarizing pulses from −40 to −10 mV were also increased progressively and then reduced to the baseline, whereas inward currents in response to hyperpolarizing pulses to −110 mV (more negative than the normal resting potential) were decreased in amplitude monotonically (not illustrated). These findings indicate that both outward and inward ACh-induced K^+ currents can be altered by intracellular Mg^{2+}.

Macroscopic current–voltage relationships were determined in another series of experiments as the difference of currents elicited before and during the application of various concentrations of ACh. Figure 2*A* shows representative current traces

before (*Aa*) and during 10^{-6} M-ACh (*Ab*) with 1 mM-Mg^{2+} in the pipette solution. Each panel is comprised of original traces recorded during test pulses to 0 mV (upper traces) and −80 mV (lower traces) from the holding potential of −40 mV. Figure 2*Ac* shows traces after application of 10^{-6} M-ACh in the absence of Mg^{2+}. The pipette always contained 0·1 mM-GTP. Current–voltage relationships in these three different

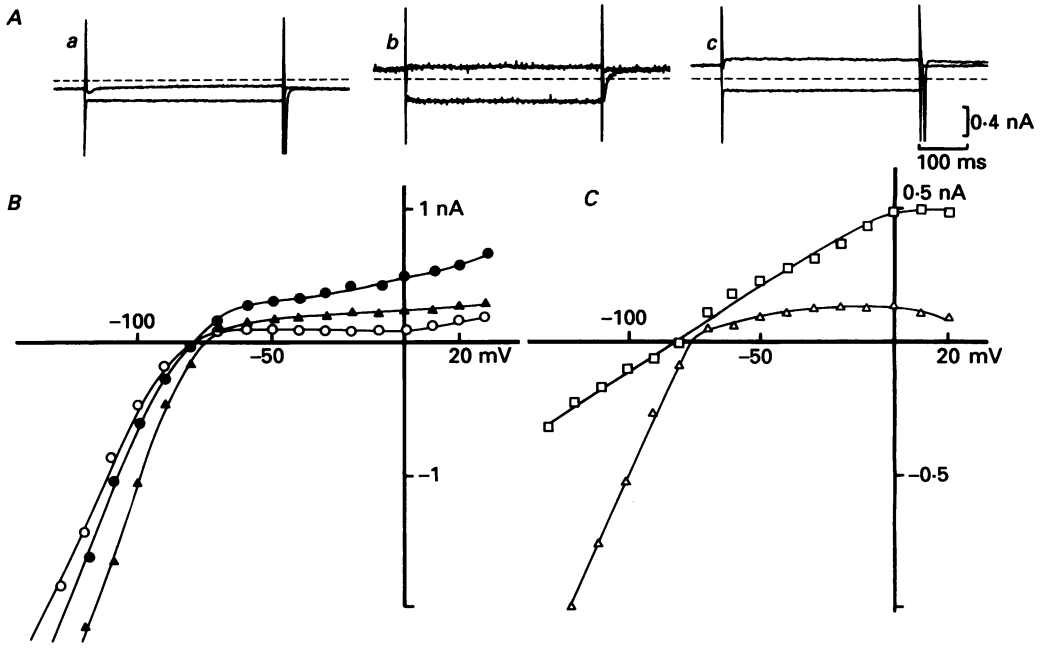

Fig. 2. Effects of intracellular Mg^{2+} depletion on muscarinic K^+ current. *A*, voltage-clamp records from the holding potential of −40 mV to test potentials of 0 mV (upper traces) and −80 mV (lower traces). The small inward current upon depolarization in *Aa* is a remnant of Ca^{2+} current despite the presence of 2μM-D600 and the large tail currents after the test pulses of −80 mV (*Aa*, *b*, *c*) are presumably due to activation of Na^+ current. Dashed lines indicate the zero current level. *B*, current–voltage relationships obtained before (○) and during (●, ▲) 10^{-6} M-ACh exposure. The cell was different from that of Fig. 1. The filled triangles indicate currents recorded with pipette solution containing 0·1 mM $[GTP]_i$ and 1 mM $[Mg^{2+}]_i$, and the filled circles those after elimination of $[Mg^{2+}]_i$. *C*, difference currents, i.e. ACh-induced currents, before and after Mg^{2+} withdrawal are plotted against membrane potential. Open triangles show results at 1 mM $[Mg^{2+}]_i$ and open squares at nominally zero $[Mg^{2+}]_i$.

conditions are illustrated in Fig. 2*B*. ACh-induced currents in the presence (△) and absence (□) of intracellular Mg^{2+} are plotted against membrane potentials in Fig. 2*C*.

These ACh difference current–voltage relationships reveal that in the absence of Mg^{2+} the conductance for inward currents was smaller, but that for outward currents was larger, than in the presence of 1 mM-Mg^{2+}. As a result, an ohmic conductance was observed between −120 and +10 mV with nominally Mg^{2+}-free pipette solution. It was also noted that the noise level of both outward and inward currents became more

prominent when measured with 1 mM-Mg^{2+} pipette solution (Fig. 2*Ab*). Similar results were obtained consistently in five other experiments.

These results indicate that Mg^{2+} increased conductance at potentials negative to the resting potential, but lowered conductance at potentials positive to it, thereby causing inward rectification of ACh-sensitive currents.

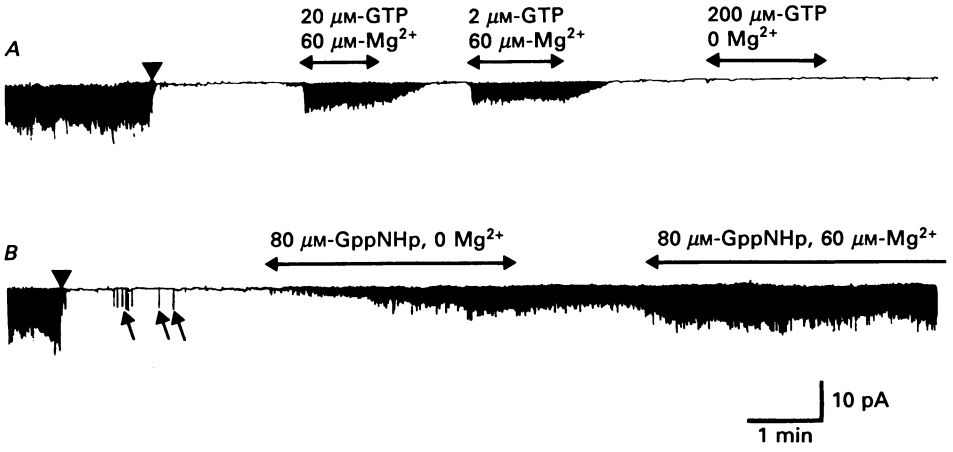

Fig. 3. Run-down of the muscarinic K^+ channel and the recovery by guanine nucleotides. The patch electrodes contained the standard 150 mM-K^+ pipette solution (Table 1) and 5×10^{-6} M-ACh. The cells were superfused with a 150 mM-K^+ internal solution. In both *A* and *B*, at the time indicated by the arrow-heads, inside-out patch mode was established. Openings of ATP-sensitive K^+ channel are seen since the internal solution does not contain ATP (small arrows in panel *B*). The channel was reactivated by an application of GTP (*A*) or of the non-hydrolysable GTP analogue, GppNHp (*B*). Compositions of the internal (bath) solutions are indicated above the current traces. The holding potential was −60 mV in *A* and *B*. Time and current calibrations are given to the right of panel *B*.

Single muscarinic K^+ channel currents in cell-free patches

To further investigate mechanisms underlying these dual actions of Mg^{2+} on the muscarinic K^+ conductance, single-channel currents were recorded in the inside-out patch mode, so that concentrations of Mg^{2+} and GTP at the internal side of the patch membrane ($[Mg^{2+}]_i$ and $[GTP]_i$) could be easily controlled. Figure 3*A* depicts a slow chart record of inward single muscarinic K^+ channel currents in a cell-attached patch, measured at −60 mV, using the standard pipette solution (150 mM-KCl) containing 5×10^{-6} M-ACh. The resting potential was assumed to be zero, since the cell was superfused with a Ca^{2+}-free, 150 mM-KCl solution (standard internal solution; Table 1).

Immediately after excising the patch (inside-out mode, marked by arrow-head in the figure), the channel activity disappeared, despite the continued presence of ACh in the patch pipette (run-down). Micromolar concentrations of GTP applied internally (added to a bath solution in this condition) led to the reappearance of channel activity in the presence of micromolar $[Mg^{2+}]_i$. In the absence of intracellular Mg^{2+}, however, there was no channel activation, even by 0·2 mM-GTP (Fig. 3*A*). In

contrast, a non-hydrolysable GTP analogue, GppNHp, restored channel activity at nominally zero $[Mg^{2+}]_i$ (Fig. 3*B*). Moreover, once the channel was reactivated by GppNHp, the channel activity lasted for more than 10 min with no obvious run-down even after removal of GppNHp from the inner side of the patch membrane, as already noted (Horie & Irisawa, 1987). The above finding suggests that GppNHp

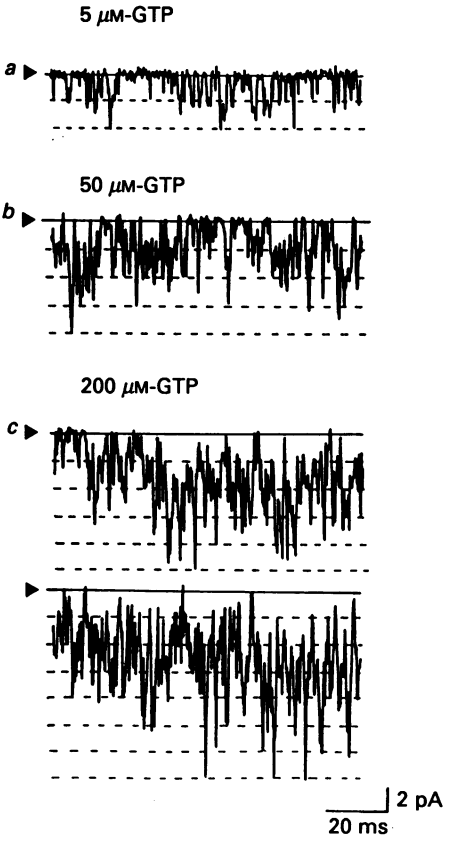

Fig. 4. Higher time resolution current traces recorded while various concentrations of GTP were applied to the internal surface of an inside-out patch membrane ($[GTP]_i$, Fig. 3*A*): *a*, 5 μM; *b*, 50 μM and *c*, 200 μM $[GTP]_i$ in the presence of 0·3 mM $[Mg^{2+}]_i$. Arrow-heads and continuous lines indicate the zero current level and dashed lines the unitary amplitude of open-channel currents (*i*). $[K^+]_i = [K^+]_o = 150$ mM, holding potential was −60 mV, and sample time was 0·2 ms. Current and voltage calibrations are given to the right of the lower trace.

should be a useful pharmacological tool to allow examination of the effects of intracellular Mg^{2+} on the single-channel conductance, since the $[Mg^{2+}]_i$ can be quantitatively controlled, while avoiding the run-down phenomenon.

The single-channel properties at relatively high $[Mg^{2+}]_i$, examined with a faster sweep (Fig. 4), coincided well with those recorded in the cell-attached mode and showed good agreement with the single-channel conductance reported by other authors (42 pS at symmetrical 150 mM-K^+ solutions) (Sakmann *et al.* 1983; Soejima

& Noma, 1984). On increasing $[GTP]_i$ from 5 μM to 0.2 mM, the inward current through single muscarinic K^+ channels (mean patch current: $\bar{i} = NPi$) increased (Fig. 4). The unitary amplitude (i) remained unchanged, the product of the number of channels and the open probability (NP) increased.

Muscarinic K^+ currents are $[GTP]_i$- and $[Mg^{2+}]_i$-dependent

To evaluate quantitatively the single-channel activation by GTP, mean inward patch currents were calculated every 2 s from the current data obtained at various intracellular GTP concentrations, in the presence of 0·33 mM $[Mg^{2+}]_i$. Figure 5 shows typical results. The mean patch current clearly increased with an increase in $[GTP]_i$. Since the single-channel current level fluctuated considerably (Fig. 5*A*, see also Fig. 4), the average of the mean patch current sampled over 30 s was plotted against $[GTP]_i$ (Fig. 5*B*). The GTP-dependent channel activation was increased from 0·2 to 5·5 pA on raising $[GTP]_i$ from 2 μM to 2 mM. The relationship between the mean patch current and $[GTP]_i$ could be expressed by saturation kinetics as follows:

$$\bar{i} = \frac{\bar{i}_{max}}{1 + (K_h/[GTP]_i)^n}, \quad (1)$$

where $\bar{i}_{max}$ is the maximal mean patch current (5·5 ± 0·3 pA). The smooth line in the graph was drawn using eqn (1) with a Hill coefficient (n) of 1. The half-saturation concentration (K_h) of $[GTP]_i$ was 31 μM. The dotted line indicates the current level measured from the same patch in the cell-attached patch mode before establishing the inside-out mode. The line crosses the dose–response curve at $[GTP]_i = 85$ μM. Assuming that the regulation of the channel by GTP is independent of other soluble cytosolic substances, endogenous GTP concentrations would be around 85 μM in this cell. The average (± S.D.) of endogenous GTP concentration, estimated under similar conditions in four experiments, was 106 ± 23 μM and the dose–response curves gave Hill coefficients of 1 and K_h values of 24 ± 8 μM.

The effects of $[Mg^{2+}]_i$ on mean inward patch current in the constant presence of 2 μM $[GTP]_i$ were examined in five different patches. Mean patch currents (NPi) were normalized with respect of those recorded at 2 mM $[Mg^{2+}]_i$ in each patch and are plotted against $[Mg^{2+}]_i$ (Fig. 6*A*). With increasing $[Mg^{2+}]_i$, the channel availability was increased. The relationship between normalized mean patch current (NP) and $[Mg^{2+}]_i$ could be approximated by saturation kinetics as follows:

$$\bar{i} = \frac{\bar{i}_{max}}{1 + (K_d/[Mg^{2+}]_i)^n}, \quad (2)$$

where K_d was 67 ± 14 μM and n was 1 (five experiments). It was concluded that $[Mg^{2+}]_i$ showed a one-to-one relationship for eliciting K^+ current, possibly through activation of a GTP-binding regulatory protein (G protein).

In the next series of experiments, the correlation between $[Mg^{2+}]_i$ and $[GTP]_i$ effects on channel activation was examined in a single patch (Fig. 6*B*). The mean patch currents were normalized with respect of those measured at 1 mM $[GTP]_i$ and 0·33 mM $[Mg^{2+}]_i$. At 3·45 μM $[Mg^{2+}]_i$ (lower curve), the channel activation was about one-fifth of that obtained at 0·33 mM $[Mg^{2+}]_i$ (upper curve). The hundredfold change in $[Mg^{2+}]_i$, however, did not markedly shift the K_h value of the $[GTP]_i$–response

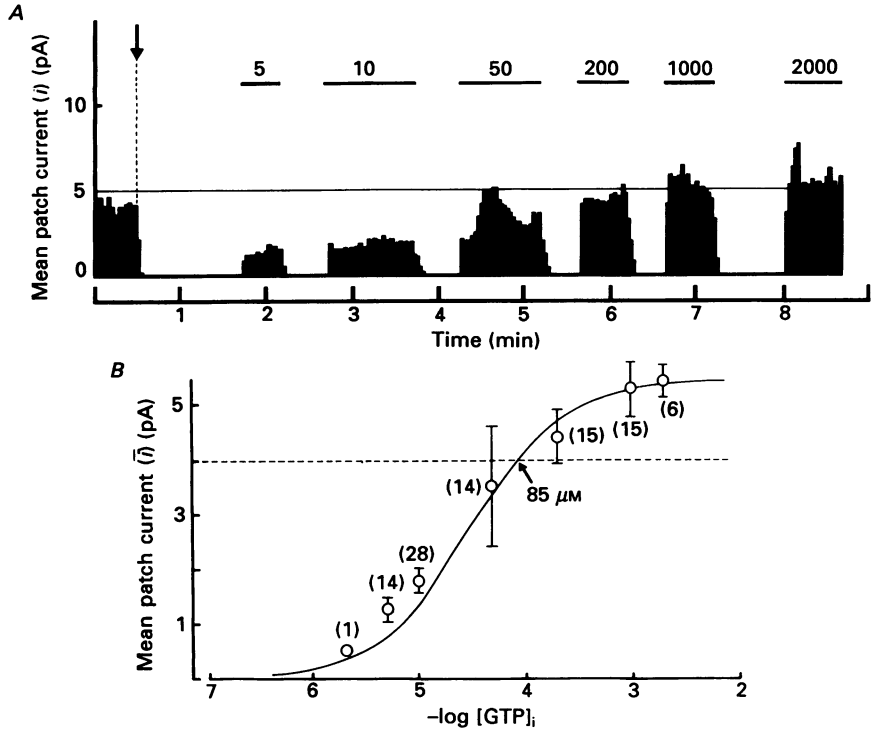

Fig. 5. Relationships between internal GTP level and inward muscarinic K^+ current activation with symmetrical K^+ concentrations. *A*, mean inward patch current ($\bar{i}$) at the holding potential of −80 mV was calculated every 2 s from the current records at various intracellular GTP concentrations (indicated at the top of the figure in μM), and the distribution against time is displayed in the bar graphs. At the time indicated by the arrow, the patch was excised into the standard internal solution (Table 1) containing 0·33 mM-Mg^{2+}. This concentration of Mg^{2+} was present throughout the experiment. *B*, mean patch currents, calculated at a given $[GTP]_i$ (in M) in *A*, are plotted as a function of $[GTP]_i$. The data were sampled every 2 s for longer than 30 s (dwell time of 0·2 ms) and sample number at each $[GTP]_i$ is given beside each point. Vertical bars indicate the standard deviations of mean patch currents. The smooth line was drawn using the eqn (1). The dashed horizontal line indicates the mean patch current in the cell-attached patch mode measured before the inside-out mode was started (sample number of 16).

relationship (K_h was 13 and 24 μM, respectively). Similar results were obtained in two other patches. Thus, raising $[Mg^{2+}]_i$ enhanced further the channel activity that was resumed at maximal $[GTP]_i$ (e.g. 1 mM). Taken together, the results shown in Fig. 6*A* and *B* indicate that the effects of intracellular Mg^{2+} on channel activation appear to be additive with those of intracellular GTP, thus suggesting that there are two different binding sites on the G proteins, one for GTP and one for Mg^{2+}.

Multiple conductance levels of muscarinic K^+ channels

The three panels of Fig. 7 show successive current traces recorded at a higher time resolution in the presence of 2 μM $[GTP]_i$ and 0·33 mM $[Mg^{2+}]_i$. Unitary channel openings appeared as brief rectangular pulses of 2·4 pA at −60 mV, but often showed

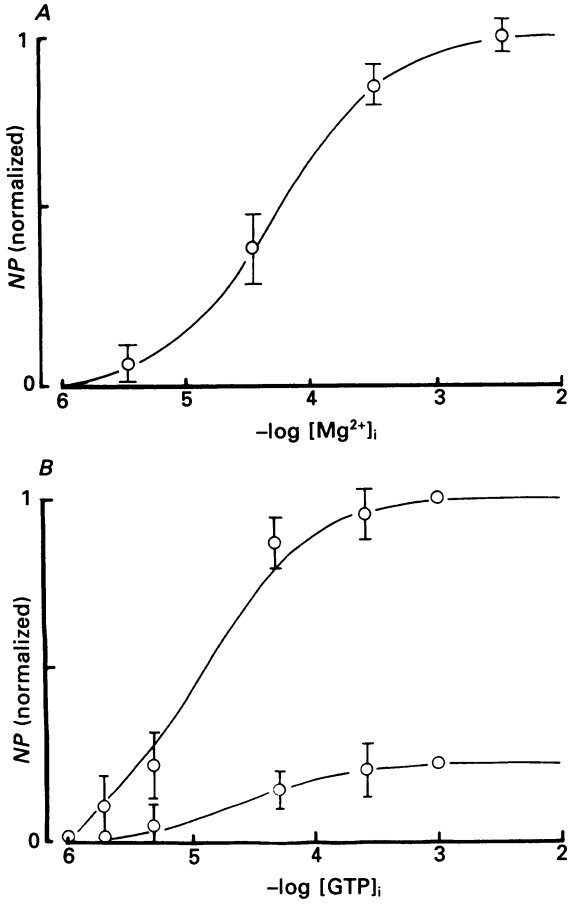

Fig. 6. Effects of Mg^{2+} applied internally on inward muscarinic K^+ currents in symmetrical K^+ solutions. *A*, throughout this experiment, 2μM $[GTP]_i$ was present in the inside-out mode. The holding potential was −80 mV. The mean inward patch current (*NPi*) at four different intracellular Mg^{2+} concentrations, measured as described in Methods and Fig. 5, was normalized to that recorded at 2 mM $[Mg^{2+}]_i$. Vertical bars are the standard deviations in five different patches. The curve was drawn using eqn (2). *B*, within a single experiment, the effects of changing $[Mg^{2+}]_i$ on the GTP activation of muscarinic K^+ current were examined at two intracellular Mg^{2+} concentrations (lower curve, 3·45μM; upper curve, 0.33 mM). Holding potential was −80 mV. Mean inward patch currents at a given $[GTP]_i$ were normalized to that recorded at 1 mM $[GTP]_i$ and 0·33 mM $[Mg^{2+}]_i$, and are plotted as a function of $[GTP]_i$. Vertical bars show the standard deviations determined from twenty to forty consecutive sets of data sampled every 2 s. The lines were drawn according to eqn (1).

abrupt interruptions to one-third (13·3 pS) or two-thirds (26·6 pS) of the unitary amplitude, as indicated by arrows. These reveal the presence of sub-conductance states, a phenomenon now known to occur in a variety of K^+ channels, e.g. serotonin-sensitive K^+ channels of *Aplysia* sensory neurones (Siegelbaum, Camardo & Kandel, 1982), Ca^{2+}-activated K^+ channels in cultured rat muscle (Barret, Magleby & Palotta, 1982), K^+-selective channels of renal tubules of *Amphiuma* (Hunter &

Giebisch, 1987), inwardly rectifying K^+ channels of mammalian heart cells (Kameyama, Kiyosue & Soejima, 1983; Sakmann & Trube, 1984; Matsuda, 1988), and Na^+-activated K^+ channels of guinea-pig ventricular cells (M. Horie & H. Irisawa, unpublished observations). In the cell-attached patch mode, brief sub-conductance states also appeared when the concentration of agonist (ACh) was extremely low (10^{-9}–10^{-10} M). At higher ACh or intracellular GTP concentrations, however, the availability of sub-conductance states was presumably low, since the sublevels were then no longer evident.

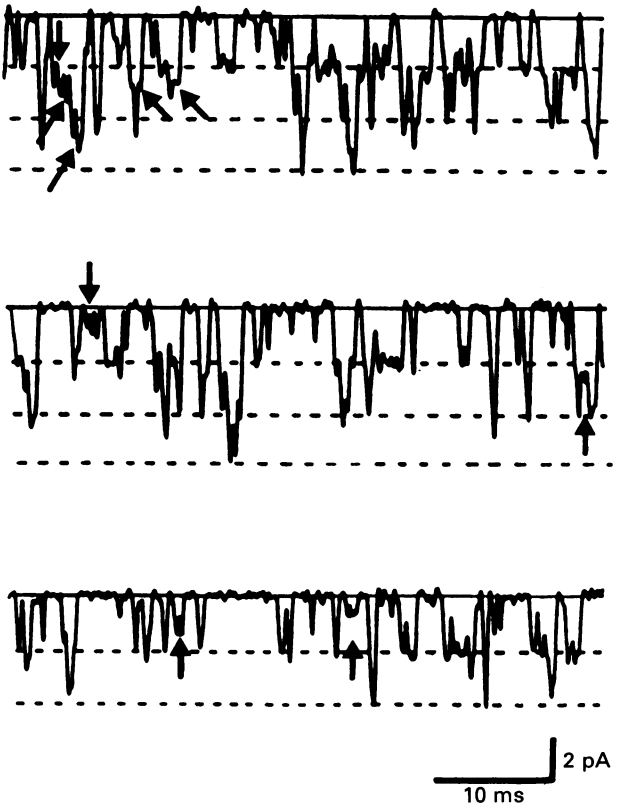

Fig. 7. Three higher-speed traces of inward currents, showing the presence of two sub-conductance states with brief transitions to one- or two-thirds of the full opening (2·4 pA, indicated by small arrows) at the membrane potential of −60 mV. Sample time was 50 μs, with cut-off frequency of 10 kHz. Continuous lines refer to the zero current level and dotted lines to the unitary amplitude of open-channel currents (i). $[K^+]_i = [K^+]_o =$ 150 mM, $[GTP]_i = 2$ μM, and $[Mg^{2+}]_i = 0{\cdot}33$ mM.

Single-channel conductance of GTP- and Mg^{2+}-dependent channels

The dependence on membrane potential of the unitary amplitude of single-open-channel current (i) was examined in inside-out patches by using micromolar GppNHp to restore channel activity at nominally zero $[Mg^{2+}]_i$ (see Fig. 3*B*). Under these conditions, we were able to evaluate the effects of various extracellular K^+ concentrations ($[K^+]_o$) on the outward current, in the absence of Mg^{2+} blockade, a

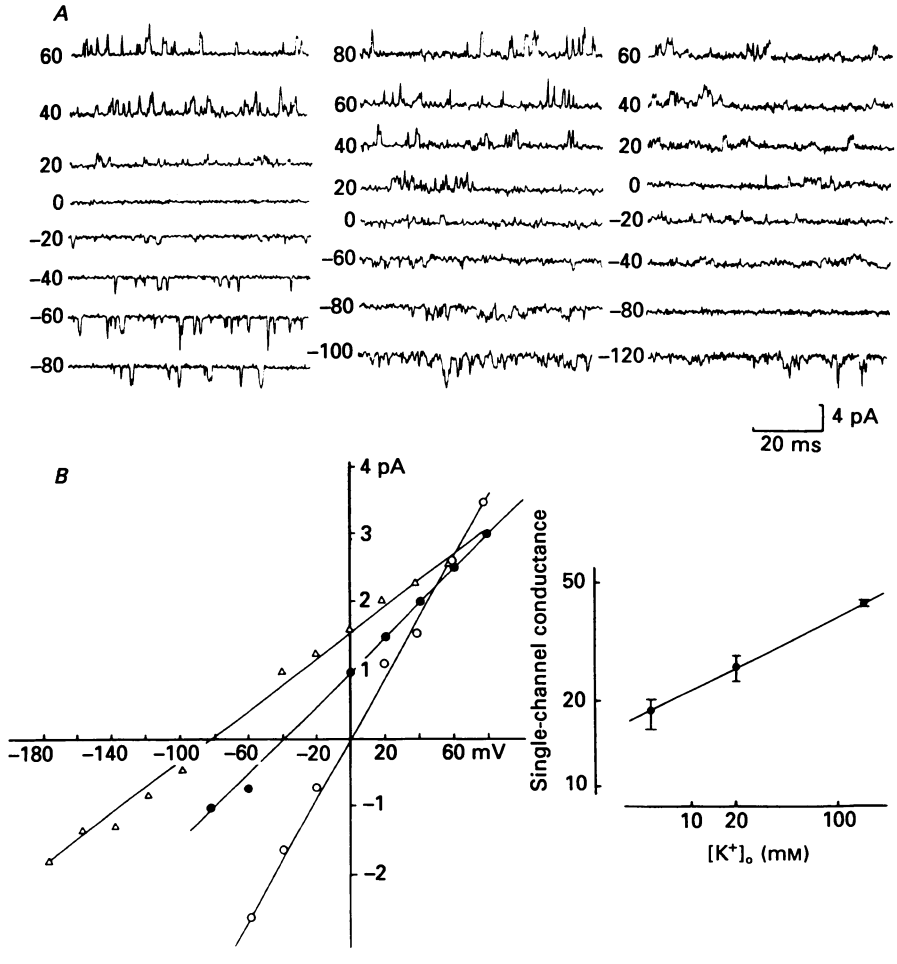

Fig. 8. Ohmic conductance of the muscarinic K^+ channel. *A*, original current traces measured in the inside-out patch mode at nominally zero $[Mg^{2+}]_i$ and 150 mM $[K^+]_i$, and with pipette solutions containing three different extracellular K^+ concentrations: 150 mM (left column), 20 mM (middle column), and 5·4 mM (right column). 0·1 mM-GppNHp was used to recover the channel. *B*, single-channel current–voltage relationships at nominally zero $[Mg^{2+}]_i$, 150 mM $[K^+]_i$, and three different levels of $[K^+]_o$. ○, 150 mM; ●, 20 mM and △, 5·4 mM $[K^+]_o$. *C*, log–log plot of single-channel conductance (γ) as a function of $[K^+]_o$. The straight line was drawn according to the equation: $\gamma = 13{\cdot}3\ ([K^+]_o)^{0{\cdot}23}$ (pS). Vertical bars through each point indicate the standard deviation.

condition we previously used in the whole-cell clamp mode (see Figs 1 and 2). Figure 8*A* shows some results from such an experiment conducted at three different $[K^+]_o$ levels of 150, 20, and 5·4 mM, respectively. The three single-channel current–voltage relations measured in this way (Fig. 8*B*) reversed close to the calculated K^+ equilibrium potentials ($E_K = 0$, -49, and -83 mV, respectively; 25 °C) and were virtually linear between -180 and $+80$ mV. Raising $[K^+]_o$ increased the single-channel conductances (γ) at nominally zero $[Mg^{2+}]_i$. Average values (±S.D.) for γ

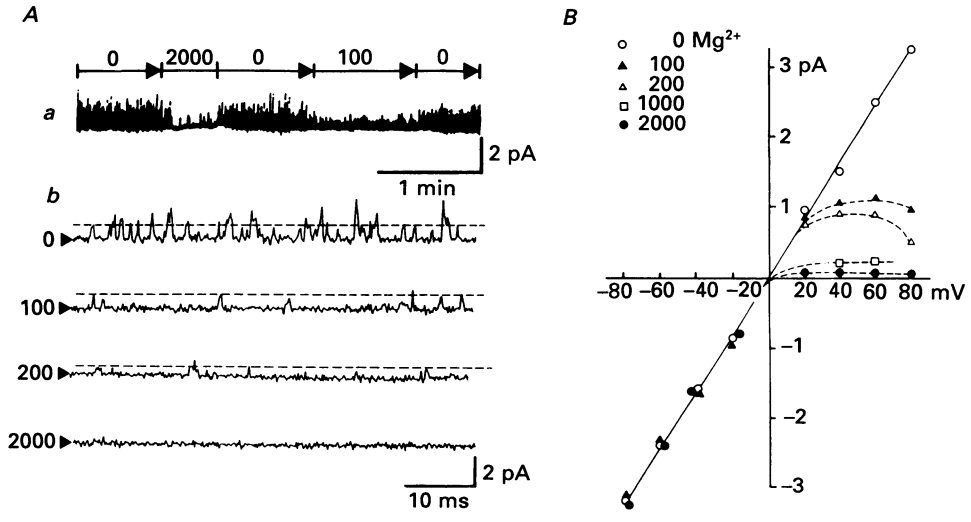

Fig. 9. Voltage- and dose-dependent Mg^{2+} block of outward muscarinic K^+ currents. *Aa*, original chart record measured in the inside-out patch mode, at the holding potential of +40 mV with symmetrical 150 mM-K^+ solutions. The channel availability was restored by 0·1 mM-GppNHp. Numbers at the top of the graph indicate $[Mg^{2+}]_i$ levels (in μM). *Ab*, four high-speed traces recorded at 0, 100, 200 and 2000 μM $[Mg^{2+}]_i$ (holding potential of +40 mV). Arrow-heads to the left of each trace indicate the zero current level and dashed lines the unitary amplitude of open-channel current (*i*). Low-pass filter was set at 3 kHz (sample time of 0·1 ms). *B*, single-channel current–voltage relationships at five different $[Mg^{2+}]_i$. Symbols: ○, 0; ▲, 100; △, 200; □, 1000; ●, 2000 μM $[Mg^{2+}]_i$. 0·1 mM-GppNHp was continuously present.

determined in *n* experiments were: 41±2 pS at 150 mM $[K^+]_o$ ($n = 7$), 26±3 pS at 20 mM $[K^+]_o$ ($n = 3$), and 18±2 pS at 5·4 mM $[K^+]_o$ ($n = 5$). As shown in the log–log plots of Fig. 8*C*, the data could be fitted by a straight line with a slope of 0·23.

Voltage-dependent and unidirectional Mg^{2+} block of GTP- and Mg^{2+}-activated channels

As shown in the slow chart record of Fig. 9*Aa*, raising $[Mg^{2+}]_i$ reduced outward K^+ currents (cf. Fig. 2), whereas it increased inward K^+ currents as already shown in Figs 3*B* and 6*A*, again illustrating the dual effect of $[Mg^{2+}]_i$ on muscarinic K^+ channels. Records at a higher time resolution (Fig. 9*Ab*) reveal that $[Mg^{2+}]_i$ reduced both the unitary amplitude and the open probability of *outward* K^+ channel current in a dose-dependent manner. On the other hand, the unitary *inward* open-channel current was of normal amplitude even in the presence of a relatively high $[Mg^{2+}]_i$ (Fig. 9*B*) and the open probability (*NP*) was markedly enhanced by high $[Mg^{2+}]_i$ (Fig. 6*A*). The action of $[Mg^{2+}]_i$ to reduce the unitary current amplitude was therefore unidirectional. In contrast, Mg^{2+} in the pipette (extracellular Mg^{2+}) had no effect on muscarinic K^+ currents, either inward or outward.

Single-channel current–voltage relationships at zero $[Mg^{2+}]_i$, and at four different levels of $[Mg^{2+}]_i$, are shown in Fig. 9*B*. The chord conductances for the outward current became smaller at membrane potentials positive to E_K and produced

negative slopes of the current–voltage relations at 100 and 200 μM $[Mg^{2+}]_i$, suggesting that Mg^{2+} block of the channel is voltage-dependent. These findings are consistent with the concept that Mg^{2+} acts as a fast open-channel blocker by readily entering the aqueous channel pore via its internal orifice, but cannot proceed over the energy barrier between the Mg^{2+} binding site and the external opening of the channel, thereby preventing K^+ passage.

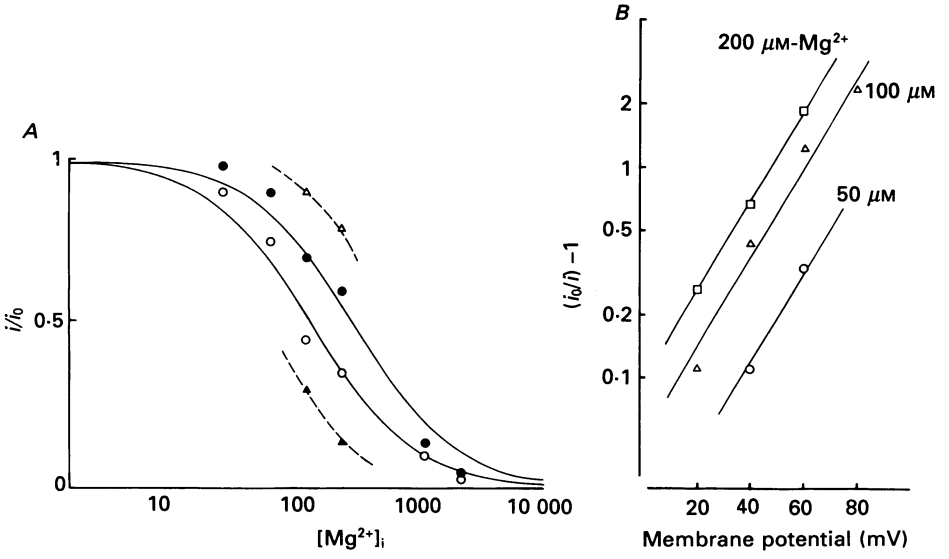

Fig. 10. Voltage dependence of Mg^{2+} block. *A*, unitary open-channel currents (i), normalized by referring to that measured at nominally zero $[Mg^{2+}]_i$ (i_0), are plotted against $[Mg^{2+}]_i$ on a semilogarithmic scale. Smooth curves were derived from eqn (3), with a Hill coefficient of 1 and K_b of 250 μM at +40 mV and 111 μM at +60 mV, respectively. Dashed curves through the data at +20 and +80 mV were drawn by eye. Symbols: △, +20 mV; ●, +40 mV; ○, +60 mV; ▲, +80 mV. *B*, determination of the voltage dependence of Mg^{2+} block (δ). Parallel lines were fitted to semilogarithmic plots of $(i_0/i)-1$ against the membrane potential, thereby giving the electrical fraction of Mg^{2+} binding site, $\delta = 0{\cdot}64$ in this experiment, based on eqn (5).

The unitary amplitude (i) of outward current at a given $[Mg^{2+}]_i$ was normalized to that obtained at nominally zero $[Mg^{2+}]_i$ (i_0), and the ratio (i/i_0) so calculated over the range of membrane potentials between +20 and +80 mV is plotted against $[Mg^{2+}]_i$ in Fig. 10*A*. The resulting relationships were well accounted for by saturation kinetics, as previously shown for the ATP-sensitive K^+ channel of guinea-pig ventricular cells (Horie *et al.* 1987):

$$i/i_0 = \frac{1}{1+([Mg^{2+}]_i/K_b)^n}, \tag{3}$$

where K_b is the half-blocking dose of intracellular Mg^{2+} and the Hill coefficient (n) is 1. On the basis of Eyring rate theory (Woodbury, 1971; Hille, 1984), K_b is expected to be a function of membrane potential (E_m):

$$K_b = K'_b \exp(z\delta E_m F/RT), \tag{4}$$

where K'_b is the value of K_b at 0 mV, δ represents the fractional electrical distance between the internal mouth of the channel pore and the Mg^{2+} binding site, and z is the valency of the blocking particle (in this instance, $z = 2$). F, R and T have their usual meaning. The values of K_b, calculated on the basis of eqn (3), shifted to lower concentrations at more positive potentials and were 293 ± 31 μM at $+40$ mV and 115 ± 9 μM at $+60$ mV, respectively (four experiments).

To quantify the voltage dependence of the Mg^{2+} block, eqns (3) and (4) were rearranged as follows:

$$\ln((i_0/i)-1) = \frac{z\delta E_m F}{RT} + \ln\frac{[Mg^{2+}]_i}{K'_b}.$$

As shown in Fig. 10*B*, $\ln((i_0/i)-1)$ was plotted against normalized membrane potential (zE_mF/RT) at different levels of $[Mg^{2+}]_i$. The slopes of the fitted parallel lines gave values for the fractional electrical distance of the Mg^{2+} binding site (δ) of $0{\cdot}63 \pm 0{\cdot}05$ (four experiments).

DISCUSSION

Biochemical aspects of intracellular Mg^{2+} action

Two major findings emerge from our study:

(1) Intracellular Mg^{2+} facilitates the coupling of G proteins to the muscarinic K^+ channel, thereby activating channel openings in a dose-dependent manner and with little alteration in the $[GTP]_i$ dependence of channel activation. The results suggest that there may exist an additional Mg^{2+} binding site, separate from the GTP binding site, which plays a role in the coupling between G proteins and ionic channels. This is consistent with the finding, noted in *in vitro* experiments (Kurose, Katada, Haga, Haga, Ichiyama & Ui, 1986), that Mg^{2+} accelerates the dissociation of G proteins into subunits which then directly activate the muscarinic K^+ channel, although which subunit (α or $\beta\gamma$ or both) actually makes the link to the ionic channel remains an open question (Logothetis, Kurachi, Galper, Neer & Clapham, 1986; Yatani, Codina, Brown & Birnbaumer, 1987; Codina, Yatani, Grenet, Brown & Birnbaumer, 1987).

(2) Intracellular Mg^{2+} blocks the outward passage of K^+ through individual muscarinic channels in a dose- and voltage-dependent manner with the characteristics of a fast open-channel blocker, similar to recent findings for the ATP-sensitive K^+ channel and the inwardly rectifying K^+ channel (Horie *et al.* 1987; Matsuda *et al.* 1987; Vandenberg, 1987). In the present study, we found that a higher $[Mg^{2+}]_i$ increases the conductance for inward currents while decreasing that for outward currents, and thereby causes a stronger rectification of the channel.

In studies using the purified muscarinic receptors reconstituted with purified G proteins into phospholipid vesicles (Kurose *et al.* 1986), pre-treatment with pertussis toxin (islet-activating protein, IAP), a potent uncoupler of muscarinic receptor from G proteins (inhibitory and other) (Katada, Tamura & Ui, 1983), interfered with signal (carbachol) transduction, assayed as a carbachol-induced increase in the catalytic ability of G proteins as GTPase. In the same preparation treated with IAP, however, micromolar Mg^{2+} led to a resumption of the enzyme activity of G proteins. Since ADP-ribosylation by IAP prevents the dissociation of G proteins, these *in vitro*

findings suggest that Mg^{2+} itself directly enhances the splitting of G proteins, and so support the present electrophysiological results.

Biophysical aspects of intracellular Mg^{2+} action

In the regulation of muscarinic K^+ currents, the second but indispensable role of $[Mg^{2+}]_i$ is to provide a dose- and voltage-dependent block of outward currents flowing through the channel. The intracellular Mg^{2+} level at which the inward rectification of the channel occurs seems to be within the physiological range, as estimated in cardiac and skeletal muscle cells (Hess, Metzger & Weingart, 1982; Gupta, Gupta & Moore, 1984; Alvarez-Leefmans, Gamiño, Giraldez & González-Serralos, 1986; Blatter & McGuigan, 1987). The doses of Mg^{2+} required to block the outward currents in other K^+ channels of cardiac cells and pancreatic B cells are also within the physiological range (from several micromolar to several millimolar, Horie *et al.* 1987; Findlay, 1987*a*, *b*; Matsuda *et al.* 1987; Vandenberg, 1987). Thus, channel blockade due to physiological concentrations of Mg^{2+} appears to be common in cardiac K^+ channels and seems responsible for the inward rectification.

A rapid fluctuation in open-channel currents was one of the characteristics of Mg^{2+} block in the ATP-sensitive K^+ channel, and the rate constants governing the blocking kinetics were large, in the order of $10^4\ s^{-1}$ (Horie *et al.* 1987). In the muscarinic K^+ channel, during brief channel openings (mean lifetime less than 2 ms), the unitary amplitude, as well as the open probability of the channel, was reduced without increasing the current noise level in the presence of micromolar Mg^{2+}; this suggests that Mg^{2+} block of this channel has faster kinetics than those observed in the ATP-sensitive K^+ channel. Horie & Irisawa (1987) found relaxations of muscarinic K^+ currents, at the single-channel level, to have time constants of approximately 20 ms (150 mM symmetrical K^+ solution at a membrane potential of +80 mV). In whole-cell and multicellular voltage-clamp experiments (Noma & Trautwein, 1978; Osterrider, Noma & Trautwein, 1980; Iijima *et al.* 1985; Carmeliet & Mubagwa, 1986*b*), the kinetics of the muscarinic K^+ current relaxation were appreciably slower. The time course of the Mg^{2+} block is therefore too fast to account for the relaxation phenomenon of muscarinic K^+ current, suggesting that the relaxation is not caused by Mg^{2+} block.

The half-blocking doses of Mg^{2+} (K_b) appear to be smaller for channels with a smaller unitary conductance. Thus, for the muscarinic K^+ channel they were approximately one-tenth of those noted for the ATP-sensitive K^+ channel, which has a two-fold larger single-channel conductance (Horie *et al.* 1987). In the case of the inwardly-rectifying K^+ channel, precise K_b values are not available, but they seem to be even smaller than those for Mg^{2+} block of the muscarinic K^+ currents (Matsuda *et al.* 1987). These differences in K_b values may be related to the degree of rectification of the respective channel current. The electrical distance for the Mg^{2+} binding site in the muscarinic K^+ channel (δ, 0·63) was twice as large as that for the ATP-sensitive K^+ channel (0·32). Although the current block by intracellular Mg^{2+} is likely to be based on the same biophysical mechanisms, there may be differences in the properties of the Mg^{2+} binding sites among these three ionic channels.

For the maintenance of intracellular K^+ and Mg^{2+}, muscle fibres require extracellular Mg^{2+} (Alvarez-Leefmans *et al.* 1986). From the data presented here, it

can be assumed that intracellular Mg^{2+} plays a substantial role in the maintenance of cell homeostasis by preserving $[K^+]_i$. During myocardial ischaemia, the intracellular ATP level will rapidly decline (Ingwall, 1982), which in turn induces a secondary increase in $[Mg^{2+}]_i$, resulting from the release of Mg^{2+} bound to ATP. Under these circumstances, the increased $[Mg^{2+}]_i$ may cause a stronger rectification of K^+ channels and so prevent excessive loss of $[K^+]_i$ during the depolarization associated with the plateau phase of the action potential, thereby economizing a cellular metabolism.

Multiple sub-conductance states of muscarinic K^+ channels

It is of interest that two sublevel conductances of full channel opening became apparent at low levels either of exogenous GTP in the cell-free patch mode (Fig. 7) or of ACh in the cell-attached patch mode (not illustrated). The number of sub-conductance states coincided well with those observed in inwardly rectifying K^+ channels (Kameyama *et al.* 1983; Matsuda, 1988, but see also Sakmann & Trube, 1984) and in Na^+-activated K^+ channels (M. Horie & H. Irisawa, unpublished observation).

At nominally zero internal Mg^{2+}, outward currents also showed two substates with short transitions (not illustrated), similar to those illustrated in Fig. 7. The demonstration of two substates in both outward and inward channel currents indicates that the muscarinic K^+ channel may consist of three parallel and identical subunits which have a common gating mechanism, but which pass K^+ ions individually. The probability for one or two substates opening, however, seems to be slight. At higher concentrations of agonists, the overlapping of open-channel events with rapid kinetics hampered a precise examination of sub-conductance states.

Hunter & Giebisch (1987) proposed a similar structural model of a multibarrelled K^+ channel to explain three sub-conductance states of a K^+-selective channel in the apical membrane of early distal tubule in the kidney of *Amphiuma*. In their model, sub-conductance states are connected with the same rate constants governing open and closed states, and subunits operate independently, with the open probability obeying the binomial distribution. A similar two-state model was also applied during the studies on the multiple substates observed in an inwardly rectifying K^+ channel in guinea-pig heart cells (Matsuda, 1988).

Several types of independent channels, with different conductances and kinetics, have been shown to contribute to the macroscopic cardiac K^+ current, using the patch-clamp technique. Our current analyses suggest that these cardiac K^+ channels share some common characteristics such as unidirectional and voltage-dependent block by physiological levels of $[Mg^{2+}]_i$ and the presence of sub-conductance states, and that these might indicate a similarity in the chemical structure of cardiac channels at the level of their amino acid sequences.

We thank Professor C. Kawai, Kyoto University, for providing M.H. with the opportunity to work at IPS, Dr Y. Miura for his collaboration during the earlier experiments, and Dr M. Ohara, Kyushu University, for her kind comments. We also thank Dr D. C. Gadsby, Rockefeller University, for reading our revised version and giving valuable suggestions. The technical assistance of Mr M. Ohara and Mr O. Nagata is highly appreciated. This work was supported by a research grant from the Ministry of Education, Science and Culture of Japan. M.H. is a fellow of the Japan Society for Promotion of Sciences and a recipient of a Japan Heart Foundation Research Grant for 1987.

REFERENCES

ALVAREZ-LEEFMANS, F. J., GAMIÑO, S. M., GIRALDEZ, F. & GONAZÁLEZ-SERRATOS, H. (1986). Intracellular free magnesium in frog skeletal muscle fibres measured with ion-selective microelectrodes. *Journal of Physiology* **378**, 461–483.

BARRET, J. N., MAGLEBY, L. L. & PALOTTA, B. S. (1982). Properties of single calcium activated potassium channels in cultured rat muscle. *Journal of Physiology* **331**, 211–230.

BLATTER, L. A. & MCGUIGAN, J. A. S. (1986). Free intracellular magnesium concentration in ferret ventricular muscle measured with ion selective microelectrodes. *Quarterly Journal of Experimental Physiology* **71**, 467–473.

BREITWIESER, G. & SZABO, G. (1985). Uncoupling of cardiac muscarinic and β-adrenergic receptors from ion channels by a guanine nucleotide analogue. *Nature* **317**, 538–540.

CARMELIET, E. & MUBAGWA, K. (1986*a*). Changes by acetylcholine of membrane currents in rabbit cardiac Purkinje fibres. *Journal of Physiology* **371**, 201–217.

CARMELIET, E. & MUBAGWA, K. (1986*b*). Characterization of the acetylcholine-induced potassium current in rabbit cardiac Purkinje fibres. *Journal of Physiology* **371**, 219–237.

CODINA, J., YATANI, A., GRENET, D., BROWN, A. M. & BIRNBAUMER, L. (1987). The α-subunit of G_K opens atrial potassium channels. *Science* **236**, 442–445.

DUNNE, M. J. & PETERSEN, O. H. (1986). GTP and GDP activation of K^+ channels that can be inhibited by ATP. *Pflügers Archiv* **407**, 564–565.

FABIATO, A. & FABIATO, F. (1979). Calculator programs for computing the composition of the solutions containing multiple metals and ligands used for experiments in skinned muscle cells. *Journal de physiologie* **75**, 463–505.

FINDLAY, I. (1987*a*). ATP-sensitive K^+ channels in rat ventricular myocytes are blocked and inactivated by internal divalent cations. *Pflügers Archiv* **410**, 313–320.

FINDLAY, I. (1987*b*). The effects of magnesium upon adenosine-sensitive potassium channels in a rat insulin-secreting cell line. *Journal of Physiology* **391**, 611–629.

GARNIER, D., NARGEOT, J., OJEDA, C. & ROUGIER, O. (1978). The action of acetylcholine on background conductance in frog atrial trabeculae. *Journal of Physiology* **274**, 381–396.

GUPTA, R. K., GUPTA, P. & MOORE, R. D. (1984). NMR studies of intracellular metal ions in intact cells and tissues. *Annual Review of Biophysics and Bioengineering* **13**, 221–246.

HAMILL, O. P., MARTY, A., NEHER, E., SAKMANN, B. & SIGWORTH, F. J. (1981). Improved patch-clamp techniques for high-resolution current recording from the cells and cell-free membrane patches. *Pflügers Archiv* **391**, 85–100.

HESS, P., METZGER, P. & WEINGART, R. (1982). Free magnesium in sheep, ferret and frog striated muscle at rest measured with ion-selective micro-electrodes. *Journal of Physiology* **333**, 173–188.

HILLE, B. (1984). *Mechanism of Block in Ionic Channels of Excitable Membranes*. Sunderland, MA, U.S.A.: Sinauer Associates Inc.

HORIE, M. & IRISAWA, H. (1987). Rectification of muscarinic K^+ current by magnesium ion in guinea-pig atrial cells. *American Journal of Physiology* **253**, H210–214.

HORIE, M., IRISAWA, H. & NOMA, A. (1987). Voltage-dependent magnesium block of adenosine-triphosphate-sensitive potassium channel in guinea-pig ventricular cells. *Journal of Physiology* **387**, 251–272.

HUNTER, M. & GIEBISCH, G. (1987). Multi-barreled K channels in renal tubules. *Nature* **327**, 522–524.

HUTTER, O. F. & TRAUTWEIN, W. (1956). Vagal and sympathetic effects on the pacemaker fibers in the sinus venosus of the heart. *Journal of General Physiology* **39**, 715–733.

IIJIMA, T., IRISAWA, H. & KAMEYAMA, M. (1985). Membrane currents and their modification by acetylcholine in isolated single atrial cells of the guinea-pig. *Journal of Physiology* **359**, 485–501.

INGWALL, J. S. (1982). Phosphorus nuclear magnetic resonance spectroscopy of cardiac and skeletal muscles. *American Journal of Physiology* **242**, H729–744.

ISENBERG, G. & KLÖCKNER, U. (1982). Calcium tolerant ventricular myocytes prepared by preincubation in a 'KB medium'. *Pflügers Archiv* **395**, 6–18.

KAMEYAMA, M., KIYOSUE, T. & SOEJIMA, M. (1983). Single channel analysis of the inward rectifier K current in the rabbit ventricular cells. *Japanese Journal of Physiology* **33**, 1039–1056.

KATADA, T., TAMURA, M. & UI, M. (1983). The A protomer of islet-activating protein, pertussis

toxin, as an active peptide catalyzing ADP-ribosylation of a membrane protein. *Archives of Biochemistry and Biophysics* **224**, 290–298.

KURACHI, Y., NAKAJIMA, T. & SUGIMOTO, T. (1986). Role of intracellular Mg^{2+} in the activation of muscarinic K^+ channel in cardiac atrial cell membrane. *Pflügers Archiv* **407**, 572–574.

KUROSE, H., KATADA, T., HAGA, T., HAGA, K., ICHIYAMA, A. & UI, M. (1986). Functional interaction of purified muscarinic receptors with purified inhibitory guanine nucleotide regulatory proteins reconstituted in phospholipid vesicles. *Journal of Biological Chemistry* **261**, 6423–6428.

LOGOTHETIS, D. E., KURACHI, Y., GALPER, J., NEER, E. J. & CLAPHAM, D. E. (1986). The $\beta\gamma$ subunits of GTP-binding proteins activate the muscarinic K^+ channel in heart. *Nature* **325**, 321–327.

MATSUDA, H. & NOMA, A. (1984). Isolation of calcium current and its sensitivity to monovalent cations in dialysed ventricular cells of guinea-pig. *Journal of Physiology* **357**, 553–573.

MATSUDA, H., SAIGUSA, A. & IRISAWA, H. (1987). Ohmic conductance through the inwardly rectifying K^+ channel and block by internal Mg^{2+}. *Nature* **325**, 156–159.

MATSUDA, H. (1988). Open-state substructure of inwardly rectifying potassium channels revealed by magnesium block in guinea-pig heart cells. *Journal of Physiology* **397**, 237–258.

MUBAGWA, K. & CARMELIET, E. (1983). Effects of acetylcholine on electrophysiological properties of rabbit cardiac Purkinje fibers. *Circulation Research* **53**, 740–751.

NOMA, A., PEPPER, K. & TRAUTWEIN, W. (1979). Acetylcholine-induced potassium current fluctuations in the rabbit sino-atrial node. *Pflügers Archiv* **381**, 255–262.

NOMA, A. & TRAUTWEIN, W. (1978). Relaxation of the ACh-induced potassium current in rabbit sinoatrial node cell. *Pflügers Archiv* **377**, 193–200.

OSTERRIDER, W., NOMA, A. & TRAUTWEIN, W. (1980). On the kinetics of the potassium channel activated by acetylcholine in the S–A node of the rabbit heart. *Pflügers Archiv* **386**, 101–109.

PFAFFINGER, P., MARTIN, J., HUNTER, D., NATHANSON, N. & HILLE, B. (1985). GTP-binding proteins couple cardiac muscarinic receptors to a K channel. *Nature* **303**, 250–253.

SAKMANN, B., NOMA, A. & TRAUTWEIN, W. (1983). Acetylcholine activation of single muscarinic K^+ channels in isolated pacemaker cells of the mammalian heart. *Nature* **303**, 250–253.

SAKMANN, B. & TRUBE, G. (1984). Conductance properties of single inwardly rectifying potassium channels in ventricular cells from guinea-pig heart. *Journal of Physiology* **347**, 641–657.

SIEGELBAUM, S. A., CAMARDO, J. S. & KANDEL, E. R. (1982). Serotonin and cyclic AMP close single K^+ channels in *Aplysia* sensory neurones. *Nature* **299**, 413–417.

SOEJIMA, M. & NOMA, A. (1984). Mode of regulation of the ACh-sensitive K-channel by the muscarinic receptor in rabbit atrial cells. *Pflügers Archiv* **400**, 424–431.

SOROTA, S., TSUJI, Y., TAJIMA, T. & PAPPANO, A. (1985). Pertussis toxin blocks hyperpolarization by muscarinic agonists in chick atrium. *Circulation Research* **57**, 748–758.

TSIEN, R. Y. & RINK, T. J. (1980). Neutral carrier ion-selective micro-electrodes for measurement of intracellular free calcium. *Biochimica et biophysica acta* **599**, 623–638.

VANDENBERG, C. A. (1987). Inward rectification of potassium channel in cardiac ventricular cells depends on internal magnesium ions. *Proceedings of the National Academy of Sciences of the USA* **84**, 2560–2564.

WOODBURY, J. W. (1971). Eyring rate theory model of the current–voltage relationships of ion channels in excitable membrane. In *Chemical Dynamics*, pp. 601–617. New York: John Wiley & Sons.

YATANI, A., CODINA, J., BROWN, A. M. & BIRNBAUMER, L. (1987). Direct activation of mammalian atrial muscarinic potassium channels by GTP regulatory protein G_K. *Science* **235**, 207–211.

YELLEN, G. (1982). Single Ca^{2+}-activated nonselective cation channels in neuroblastoma. *Nature* **296**, 357–359.